Journal of the European Ceramic Society 23 (2003) 323–329

www.elsevier.com/locate/jeurceramsoc

Wear behavior of ceramic nozzles in sand blasting treatments

Deng Jianxin*, Feng Yihua, Ding Zeliang, Shi Peiwei

Department of Mechanical Engineering, Shandong University, Jinan 250061, Shandong Province, PR China

Received 12 February 2002; received in revised form 15 May 2002; accepted 25 May 2002

Abstract

Sand blasting nozzle is the most critical part in the sand blasting equipment. Ceramics being with high wear resistance have great potentials as the sand blasting nozzle materials. In this paper, monolithic B_4C and Al_2O_3/(W,Ti)C ceramic composite were developed to be used as nozzle materials. The wear behavior of nozzles made from these ceramic materials was compared by determining the cumulative mass loss and the erosion rates. Effect of the factors that influence the nozzle wear was investigated. Results showed that the hardness of the nozzles plays an important role with respect to its erosion wear in sand blasting processes. The monolithic B_4C nozzles being with high hardness exhibited lower erosion rates, while the Al_2O_3/(W,Ti)C nozzles with relative low hardness showed higher erosion rates under the same test conditions. Studies of the worn surface of the ceramic nozzles demonstrated that monolithic B_4C nozzles exhibited a brittle fracture induced removal process, while Al_2O_3/(W,Ti)C nozzles showed mainly a plowing type of material removal mode.

Keywords: Abrasive jet machining; Machining; Nozzles; Sand blasting; Wear resistance

1. Introduction

Sand blasting treatment is an abrasive machining process and is widely used for surface strengthening,[1] surface modification,,[2,3] surface clearing and rust removal,[1,4,5] etc. It is suitable for the treatment of hard and brittle materials, ductile metals, alloys, and non-metallic materials (e.g., germanium, silicon, glass, ceramics, and mica), and can provide perfect surface treatment to all kinds workpieces from hull, steel structure, container to watchcase, button and inject needle. In the sand blasting treatments, fine particles are accelerated in a gas stream commonly air at a few times atmospheric pressure. The particles are directed towards surfaces need to be treated. As the particles impact the surface, they cause a small fracture, and the gas stream carries both the abrasive particles and the fractured (wear) particles away. The nozzle is the most critical part in the sand blasting treatment equipment. There are many factors that influence the nozzle wear such as: the mass flow rate and impact angle,[6–9] the erodent abrasive properties,[10–12] the nozzle material and its geometry,[13–15] etc.

In sand blasting process, the material is removed primarily by repeated impact of the abrasive particles. Several studies[16,17] have been shown that impact of brittle materials by hard and sharp particles are generally thought to result from elastic/plastic fracture. This type of fracture is characterized firstly by plastic deformation of the contact area between the impacting particle and the material surface, with subsurface lateral cracks propagating outward from the base of the contact zone on the planes nearly parallel to the surface, and with median cracks propagating from the contact zone normal to the surface. The interaction of lateral and radial cracks is considered to result in material removal.

Analysis of erosion and abrasive of brittle materials typically recognizes two models of material removal: a ductile plowing type of material removal, and a fracture induced removal process. In the class of hard materials presently being considered, both processes may occur, depending on the specific stress state of the wear environment. A more brittle material may exhibit fracture induced material removal at high impact angles, but erode in a ductile fashion at low impact angles. Both types of material removal may occur simultaneously in one test since the local stress state may also vary.

Buijs[15] has noted that erosion wear can be modeled in the general form as expressed below:

$$V = AE^{n}H^{p}K_{IC}^{q} \quad (1)$$

* Corresponding author.
E-mail address: jxdeng@sdu.edu.cn (D. Jianxin).

0955-2219/02/$ - see front matter
PII: S0955-2219(02)00183-8

where V is the volume of material removed, E is the elastic modulus, H is the hardness, K_{IC} is the fracture toughness, A is a constant, and the exponents n, p, and q all depend on the model of material removal. In the case of a brittle material response, the lateral crack length that contributes to material removal is a function of the applied load. In erosion, the applied load changes during the particle impact event. However, the maximum load will occur at maximum penetration of the particle into the target, which is a function of the hardness and kinetic energy the particle loses during impact. The form of Eq. (1) deduced by Buijs for the case of erosion is given by:[15]

$$V = dE^{5/4}/\left(H_V^{17/12}K_{IC}\right) \quad (2)$$

where d is the density of the target material. In this equation the wear volume is much stronger dependence on hardness than on fracture toughness.

Since formation and propagation of the lateral and median cracks are though to be closely related to the material parameters, the wear behavior of ceramic nozzles in sand blasting processes would be successively affected by these parameters, such as: mechanical properties and microstructure. In this study, effect of the factors (such as: the nozzle material, the erodent abrasive hardness, and the abrasive grain size etc.) that influence the nozzle wear was investigated. The erosion rates of ceramic nozzles were examined in relation to its properties and the microstructure. The purpose was to characterize the effect of the properties and microstructure on the erosion wear of ceramic nozzles in sand blasting treatments.

2. Materials and experimental procedures

2.1. Preparation of the nozzle materials

The materials used for the nozzles in the present investigation were hot-pressed monolithic B_4C and Al_2O_3/(W,Ti)C ceramic composites fabricated by the authors. The average particle size of Al_2O_3 starting powders is less than 0.8 μm, and additions of (W,Ti)C particles (average particle size 1.0 μm) were added to Al_2O_3 matrix according to the combinations listed in Table 1. The average particle size of B_4C is less than 1.0 μm. The combined powders were prepared by wet ball milling in alcohol with cemented carbide balls for 80 h. Following drying, the final densification was accomplished by hot pressing with a pressure of 36 MPa in argon atmosphere for 8–60 min to produce a ceramic disk. The required sintering temperature was in the range of 1650–2150 °C.

Table 1
Composition and mechanical properties of the ceramic nozzle materials

Compositions (Vol.%)	Density (g/cm^3)	Flexural strength (MPa)	Fracture toughness (MPa $m^{1/2}$)	Hardness (GPa)
Al_2O_3/45% (W,Ti)C	6.64	850	4.9	21.5
B_4C	2.52	350	2.5	32.4

Densities of the hot-pressed ceramics were measured by the Archimedes's method. Test pieces of 3×4×36 (mm) were prepared from the disk by cutting and grinding using a diamond wheel and were offered for measurement of flexural strength, Vickers hardness and fracture toughness. A three-point bending mode was used to measure the flexural strength over a 30 mm span at a crosshead speed of 0.5 mm/min. Fracture toughness measurement was performed using indentation method in a hardness tester (ZWICK3212) using the formula proposed by Cook and Lawn.[18] On the same apparatus the Vickers hardness was measured on polished surface with a load of 98 N. Data for hardness, flexural strength, and fracture toughness were gathered on five specimens and are listed in Table 1.

2.2. Sand blasting tests

Sand blasting tests were conducted with a GS-6 sand blasting machine tool (made in China). The schematic diagram of this equipment is shown in Fig. 1. The compressed air pressure was set at 0.4 MPa. Nozzles (see Fig. 2) with internal diameter 8 mm and length 30

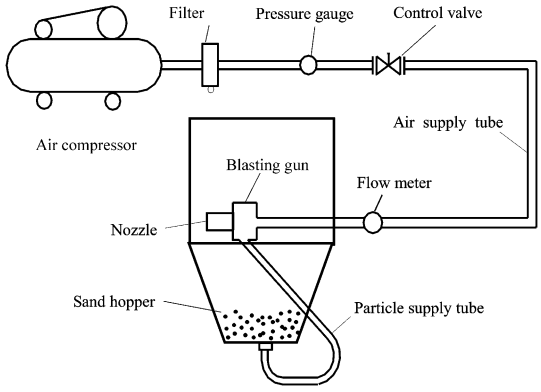

Fig. 1. Schematic diagram of the sand blasting equipment (type GS-6, made in China).

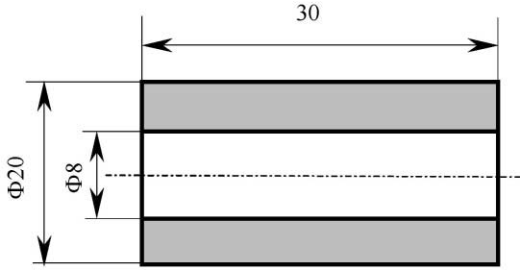

Fig. 2. Geometry and dimensions of the ceramic nozzle.

Table 2
Characterization of erodent abrasives

Abrasive	Composition	Hardness (GPa)	Density (cm^3/g)	Grit number (Mesh)	Grain size (μm)
A	$Al_2O_3 \geqslant 98.5\%$	20.0–23.0	3.95	80	180–212
B	$Al_2O_3 \geqslant 98.5\%$	20.0–23.0	3.95	60	250–300
C	$SiC \geqslant 99.0\%$	32.8–34.0	3.15	80	180–212
D	$SiC \geqslant 99.0\%$	32.8–34.0	3.15	60	250–300

mm made from monolithic B_4C and Al_2O_3/(W,Ti)C were manufactured using hot-pressing techniques. The erodent abrasives used in this study were of Al_2O_3 and SiC powders. The properties of these abrasive particles are listed in Table 2. Since the test parameters were kept constant, wear of ceramic nozzles should only depend on the nature of the nozzle and abrasive materials respectively.

The mass loss of the worn nozzles was measured with an accurate electron balance (minimum 0.1 mg). The erosion rates (W) of the nozzles are defined as the nozzle mass loss (m_1) divided by the nozzle density (d) times the mass of the erodent abrasive particles (m_2).

$$W = m_1/(d.m_2) \tag{3}$$

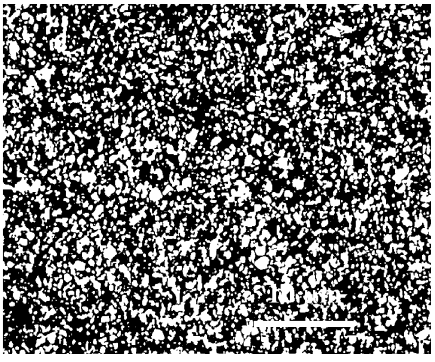

Fig. 3. Typical microstructure of the polished surface of Al_2O_3/(W,Ti)C ceramic composite.

where the W has the units of volume loss per unit mass (mm^3/g).

The fracture surfaces of the ceramic nozzle materials and the eroded bore surfaces of the nozzles were examined using scanning electron microscopy.

3. Results and discussion

3.1. Microstructural characterization of ceramic nozzle materials

Fig. 3 shows the optical micrograph of the polished surface of Al_2O_3/(W,Ti)C ceramic composite, specimens were etched using a hot-solution of phosphoric acid. In this structure, the white phase with clear contrast is of (W,Ti)C, and the gray phase is of Al_2O_3. It can be seen that the second phase was uniformly distributed with the matrix, and there were few second phase agglomerates or matrix-rich regions. Fig. 4 shows the SEM micrographs of the fracture surfaces of monolithic B_4C and the Al_2O_3/(W,Ti)C composite respectively. From these SEM micrographs, different morphologies and grain sizes of the B_4C and the composites can be seen clearly. The monolithic B_4C exhibited a flat fracture surface, resulting from the transgranular fracture mode, and there are a lot of obvious pores located at the B_4C grain boundary. A remarkable increase of the grain size (4∼8 μm) was also observed. While Al_2O_3/(W,Ti)C composite showed mainly an intergranular fracture mode, and the grain sizes were ranged from 0.5 to 1.5 μm.

3.2. Cumulative mass loss and erosion rates of the ceramic nozzles

Fig. 5 shows the cumulative mass loss of the ceramic nozzles in sand blasting process with different abrasive particles for Al_2O_3/(W,Ti)C and B_4C nozzles. It can be seen that the cumulative mass loss continuously increased with the operation time both for Al_2O_3/(W,Ti)C and B_4C

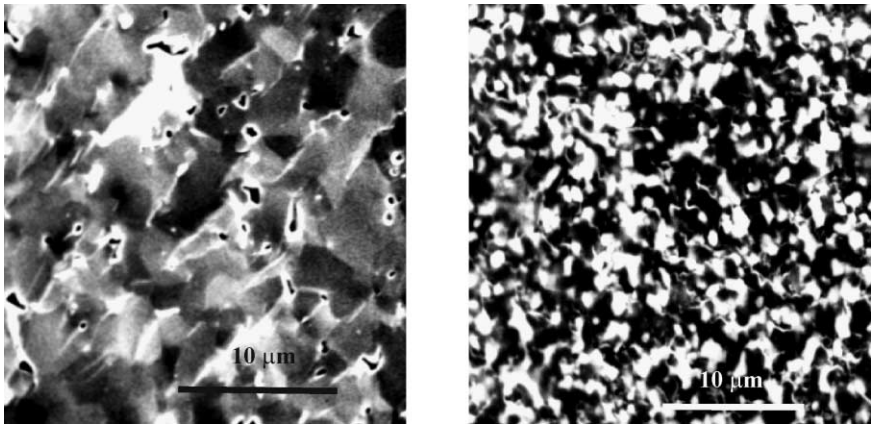

Fig. 4. SEM micrographs of the fracture surfaces of monolithic B_4C and Al_2O_3/(W,Ti)C ceramic composites.

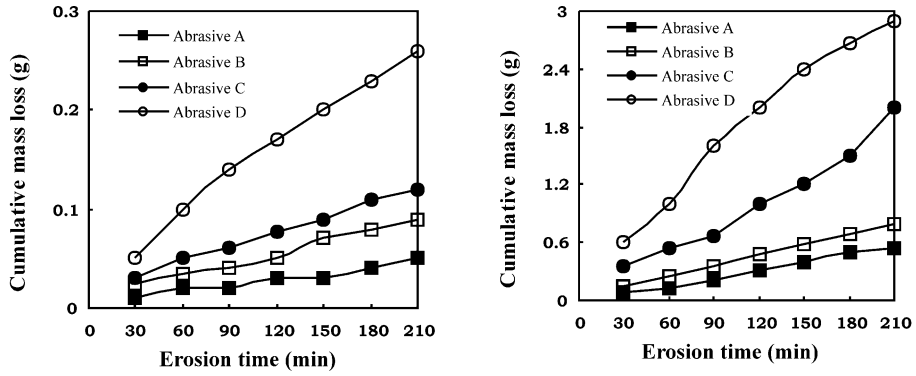

Fig. 5. Cumulative mass loss of ceramic nozzles in sand blasting processes with different abrasive particles (a) B_4C nozzles, (b) Al_2O_3/(W,Ti)C nozzles.

nozzles. As the grain size of the erodent abrasive particle increases, there is greater increase in mass loss of the ceramic nozzles. The cumulative mass loss of the nozzles is much higher when using SiC powders as the erodent abrasives. The higher the erodent abrasive grain size, the higher the cumulative mass loss of the nozzles. This can be explained by an energy consideration. The abrasive particles with smaller grain size would imply a lower impact load due to the smaller kinetic energy under identical test conditions. Therefore, the only way to put more energy into the sand blasting process is to increase the operation time (or to decrease the cumulative mass loss of the nozzles).

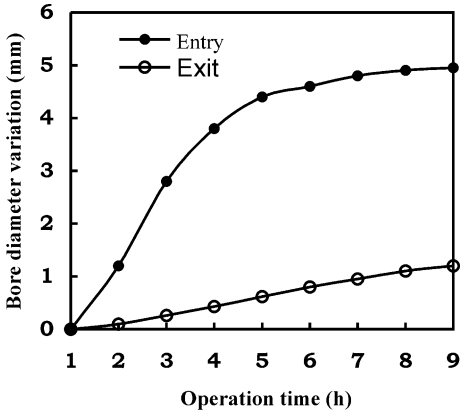

Fig. 6. Nozzle entry and exit bore diameter variation with the operation time in sand blasting processes for Al_2O_3/(W,Ti)C ceramic nozzle.

The results of the nozzle entry and exit bore diameter variation with the operation time are shown in Fig. 6 for Al_2O_3/(W,Ti)C ceramic nozzle. It can be seen that the entry bore diameter enlarges relatively fast up to 4 h operation, and within further 5 h operation it almost remains constant. At the beginning, wear in the nozzle bore entry section becomes a maximum, which may be attributed to severe impact erosion under large impact angles as can be seen in Fig. 7. After 4 h operation, a natural shape entry bore develops, and the wear mode changes from impact to sliding erosion (shallow impact or abrasion). However, the increase of the exit bore diameter follows an almost linear rate law. Fig. 8 shows the SEM micrographs of the nozzle entry bore profiles for un-worn and worn Al_2O_3/(W,Ti)C and B_4C nozzles. Form this fig. it appears that the flux is turbulent, the entry bore profile of the worn ceramic nozzle is not homogenous.

Fig. 9 shows the variation of erosion rates with the operation time for Al_2O_3/(W,Ti)C and B_4C nozzles in sand blasting process. It can be seen that the erosion rate of the nozzles showed a little decrease within the operation time both for Al_2O_3/(W,Ti)C and B_4C nozzles. The B_4C nozzles being with high hardness and low fracture toughness had smaller erosion rates, while the Al_2O_3/(W,Ti)C nozzles with high toughness and low

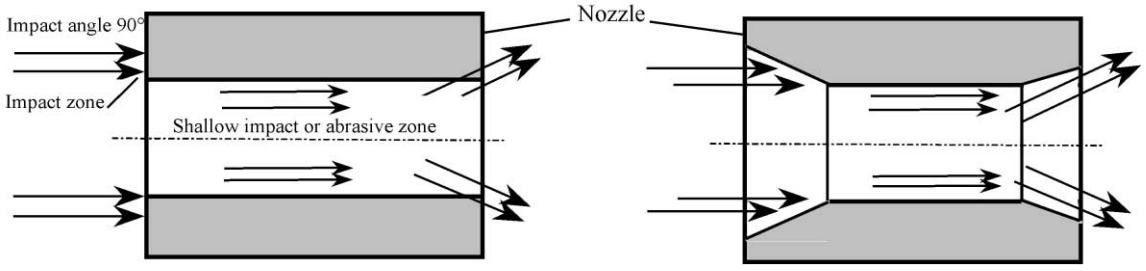

Fig. 7. Schematic diagram of the interaction between the erodent particle and the nozzle in sand blasting processes (a) at the beginning of the sand blasting process, (b) after several hours operation.

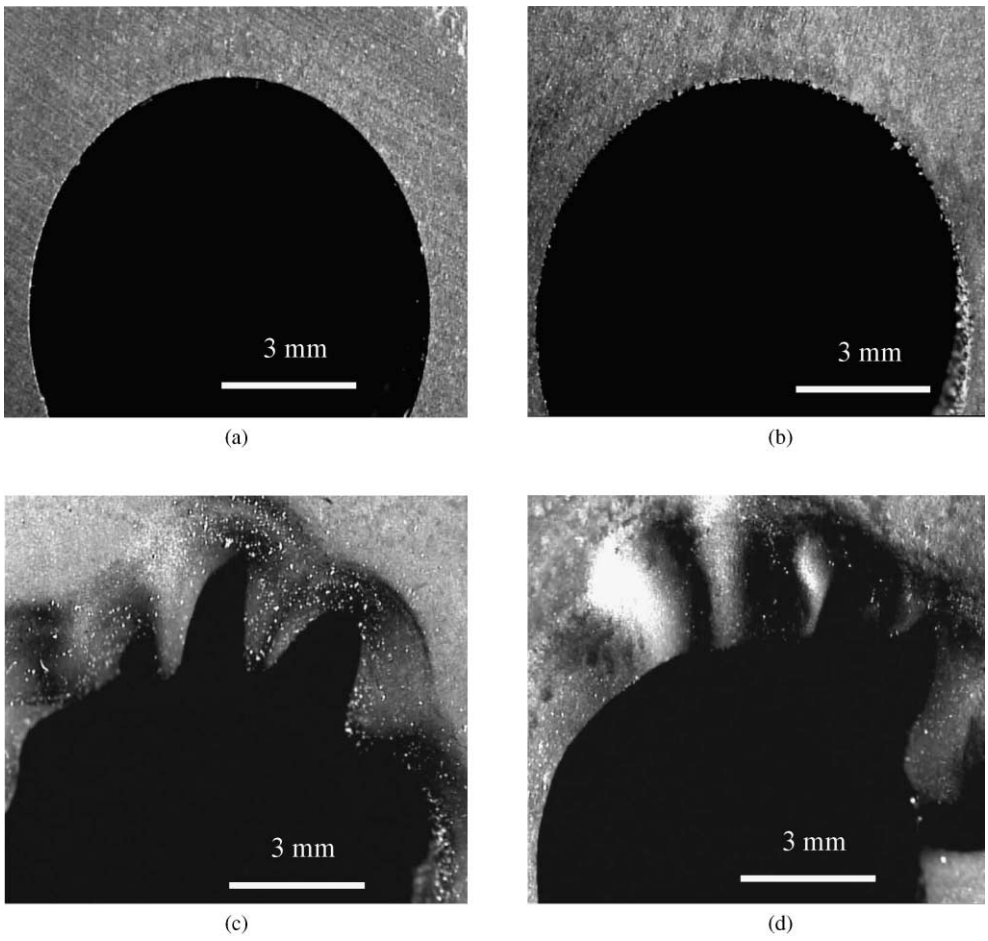

Fig. 8. Nozzle entry bore profiles of (a) un-worn Al_2O_3/(W,Ti)C nozzle, (b) un-worn B_4C nozzle, (c) worn Al_2O_3/(W,Ti)C nozzle after sand blasting for 8 h, (D) worn B_4C nozzle after sand blasting for 4 h.

hardness showed higher erosion rates. Under the same test conditions, B_4C nozzle outperforms Al_2O_3/(W,Ti)C ceramic nozzle by a factor of 4. This can be explained by the high hardness of the monolithic B_4C nozzles impacted at low angles in this sand blasting process.

Fig. 10 shows the mutual dependence of nozzle erosion rates and the hardness of erodent abrasives in sand blasting treatment. It can be seen that the abrasive particle hardness played an important role on the nozzle erosion wear. The abrasive particles with higher hardness

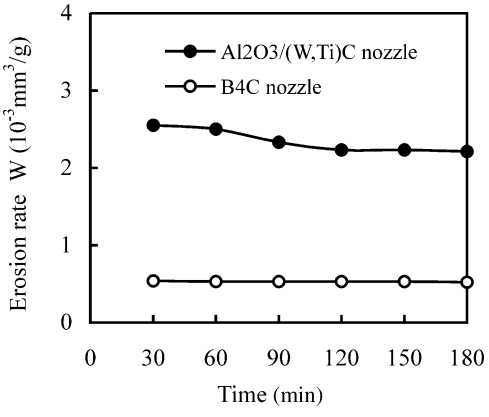

Fig. 9. Variation of nozzle erosion rates with the operation time in sand blasting process (erodent abrasive particles: SiC, abrasive grain size: 60 mesh).

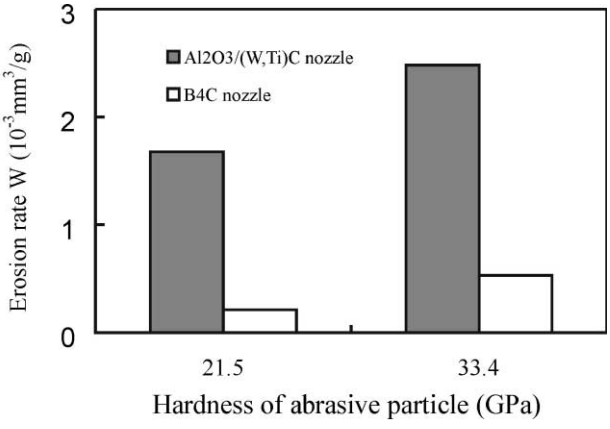

Fig. 10. Variation of nozzle erosion rates with the hardness of the erodent abrasive particles in sand blasting process (erodent abrasive particles: Al_2O_3 and SiC, abrasive grain size: 60 mesh).

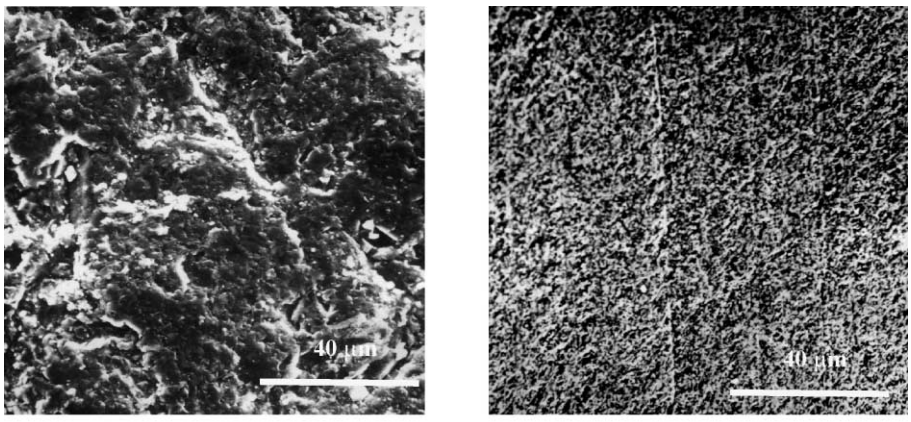

Fig. 11. SEM micrographs of the bore surfaces of the worn nozzles: (a) monolithic B_4C nozzle, (b) Al_2O_3/(W,Ti)C nozzle.

showed higher erosion rates both for Al_2O_3/(W,Ti)C and B_4C nozzles, and this effect was even greater for Al_2O_3/(W,Ti)C nozzles. The erosion rates of Al_2O_3/(W,Ti)C and B_4C nozzles continuously increased with the increasing of erodent abrasive hardness.

Fig. 11 shows the SEM micrographs of the bore surfaces of the worn B_4C and Al_2O_3/(W,Ti)C nozzles respectively. From these SEM micrographs, different morphologies and fracture modes of the monolithic B_4C and the Al_2O_3/(W,Ti)C nozzles can be seen clearly. The monolithic B_4C exhibited a brittle fracture induced removal process, resulting from the transgranular fracture mode, and there are a lot of obvious micro-cracks and small pits located on the nozzle bore surface indicating that brittle fracture took place [Fig. 11(a)]. Since the erodent particles were much softer than the B_4C, lateral cracking occurs owing to a surface fatigue mechanism. Sliding abrasive particles are also responsible for the polishing of the area between pits. While Al_2O_3/(W,Ti)C ceramic nozzles showed plowing type of material removal mode [Fig. 11(b)], and there are numerous scratches and grooves on the wear surface, which suggests that the primary wear mechanisms of the materials under these conditions is plowing and microcutting by the abrasive particles. On the flanks of the scratches and the grooves small spalling occurs. This spalling may indicate the presence of brittle fracture during chipping.

4. Conclusions

Monolithic B_4C and Al_2O_3/(W,Ti)C ceramic nozzles were produced using hot pressing techniques. The wear behavior of these ceramic nozzles in sand blasting processes was investigated. Results showed that:

1. The hardness of the nozzles plays an important role with respect to its erosion wear in sand blasting processes. The B_4C nozzles being with high hardness exhibited lower erosion rates, while the Al_2O_3/(W,Ti)C nozzles with relative low hardness showed higher erosion rates under the same test conditions.
2. The monolithic B_4C nozzles exhibited a brittle fracture induced removal process, while the Al_2O_3/(W,Ti)C nozzles showed mainly plowing type of material removal mode.
3. The erosion rates of these ceramic nozzles also depend on the hardness and grain size of the erodent abrasive in sand blasting processes. As the hardness and grain size of the erodent abrasive increases, there is dramatic increase in erosion rates of ceramic nozzles.

Acknowledgements

This work was supported by the National Science Foundation of China (Grant No. 59805012).

References

1. Guoying, Li, *Surface Engineering*. Mechanical Industry Publishing House, Beijing, 1998.
2. Jianxin, Deng and Taichiu, Lee, Techniques for improved surface integrity and reliability of machined ceramic composites. *Surface Engineering*, 2000, **16**(5), 411–414.
3. Taichiu, Lee and Jianxin, Deng, Mechanical surface treatments of EDMed ceramic composites for improved strength and reliability. *Journal of the European Ceramic Society*, 2002, **22**(4), 545–550.
4. Raykowski, A. and Hader, M., Blasting cleaning of gas turbine components: deposit removal and substrate deformation. *Wear*, 2001, **249**, 127–132.
5. Djurovic, B. and Jean, E., Coating removal from fiber composites and aluminum using starch media blasting. *Wear*, 1999, **224**, 22–37.

6. Finnie, I. and Mcfadden, D. H., On the velocity dependence of the erosion of ductile metals by solid particles at low angles of incidence. *Wear*, 1978, **48**, 181–187.
7. Oka, Y. I. and Ohnogi, H., The impact angle dependence of erosion damage caused by solid particle impact. *Wear*, 1997, **203–204**, 573–579.
8. Finnie, I., Stevick, G. R. and Ridgely, J. R., The influence of impingement angle on the erosion of ductile metals by angular abrasive particles. *Wear*, 1992, **152**, 91–97.
9. Wellman, R. G. and Allen, C., The effect of angle of impact and material properties on the erosion rates of ceramics. *Wear*, 1995, **186–187**, 117–123.
10. Srinivasan, S. and Scatterrgood, R. O. Effect of erodent hardness on erosion of brittle materials. *Wear*, **128**, 1988: 139–15.
11. Shipway, P. H. and Hutchings, I. M., The influence of particle properties on the erosive wear of sintered boron carbide. *Wear*, 1991, **149**, 85–98.
12. Bahadur, S., Badruddin, R. Erosion particle characterization and the effect of particle size and shape on erosion. In: *Proceedings of the International Conference on Wear of Materials*. ASME, New York, 1989; pp. 143–153.
13. Wood, R. J. K., Wheeler, D. W. and Lejeau, D. C., Sand erosion performance of CVD boron carbide coated tungsten carbide. *Wear*, 1999, **233–235**, 134–150.
14. Grearson, A. N., Aucote, J. and Engstrom, H., Wear of ceramics in grit blasting. *British Ceramic Transactions*, 1989, **88**, 312–318.
15. Buijs, M., Erosion of glass as modeled by indentation theory. *Journal of American Ceramic Society*, 1994, **77**, 1678–1682.
16. Lawn, B. R., Evans, A. G. and Marshall, D. B., Elastic/plastic indentation damage in ceramics: the median/radial crack system. *Journal of American Ceramic Society*, 1980, **63**(9–10), 574–581.
17. Marshall, D. B., Lawn, B. R. and Evans, A. G., Elastic/plastic indentation damage in ceramics: the lateral crack system. *Journal of American Ceramic Society*, 1982, **65**(11), 561–566.
18. Cook, R. F. and Lawn, B. R., A modified indentation toughness technique. *Journal of American Ceramic Society*, 1983, **66**(11), 200–201.